

Long-Term Depression at Parallel Fiber to Golgi Cell Synapses

Quinten Robberechts,¹ Mike Wijnants,¹ Michele Giugliano,^{1,2} and Erik De Schutter^{1,3}

¹Theoretical Neurobiology, University of Antwerp, Antwerp, Belgium; ²Brain Mind Institute, Ecole Polytechnique Fédérale de Lausanne, Lausanne, Switzerland; and ³Computational Neuroscience Unit, Okinawa Institute of Science and Technology, Okinawa, Japan

Submitted 13 January 2010; accepted in final form 17 September 2010

Robberechts Q, Wijnants M, Giugliano M, De Schutter E. Long-term depression at parallel fiber to Golgi cell synapses. *J Neurophysiol* 104: 3413–3423, 2010. First published September 22, 2010; doi:10.1152/jn.00030.2010. Golgi cells (GoCs) are the primary inhibitory interneurons of the granular layer of the cerebellum. Their inhibition of granule cells is central to operate the relay of excitatory inputs to the cerebellar cortex. Parallel fibers (PFs) establish synapses to the GoCs in the molecular layer; these synapses contain AMPA, *N*-methyl-D-aspartate (NMDA), and mostly group II metabotropic glutamate receptors. Long-term changes in the efficacy of synaptic transmission at the PF-GoC synapse have not been described previously. We used whole cell patch-clamp recordings of GoCs in acute rat cerebellar slices to study synaptic plasticity. We report that high-frequency burst stimulation of PFs, using a current-clamp or voltage-clamp induction protocol, gave rise to long-term depression (LTD) at the PF-GoC synapse. This form of LTD was not associated with persistent changes of paired-pulse ratio, suggesting a postsynaptic origin. Furthermore, LTD induction was not dependent on activation of NMDA receptors. PF-GoC LTD does require activation of specifically group II metabotropic glutamate receptors and of protein kinase A.

INTRODUCTION

The cerebellum plays an important role in several forms of motor learning. For example, there is evidence supporting the requirement of the cerebellar cortex in associative eyelid conditioning (Koekkoek et al. 2003; McCormick and Thompson 1984). Thus activity-dependent alterations in the efficacy of cerebellar synaptic transmission (i.e., potentiation, depression) are thought to underlie learning and possibly the storage of motor patterns. From early theoretical work, it was anticipated that long-term depression (LTD) at parallel fiber (PF) to Purkinje cell (PC) synapses underlies motor learning (Marr-Albus-Ito models; Albus 1971; Ito 1984; Marr 1969). Such plasticity was later experimentally shown by applying in vivo conjunctive stimulation of PFs and climbing fibers (Ito and Kano 1982). An elaborate literature exists on the synaptic plasticity of the PF-PC synapse (Jörntell and Hansel 2006; for reviews, see Ito 2001) and on plasticity at other cerebellar synapses, such as the climbing fiber to PC synapse (Coemans et al. 2004; Hansel and Linden 2000). Other synapses in the cerebellum thought to be important for motor learning are the input stage of the cerebellar cortex at the mossy fiber (MF) to granule cell (GC) synapses (D'Angelo et al. 2004) and the MF to deep cerebellar nuclei synapses, of which synaptic plasticity was also long theorized but only recently experimentally shown (Medina and Mauk 2000; Pugh and Raman 2009; Zhang

and Linden 2006). Furthermore, synaptic inputs to interneurons, such as the PF to stellate cell synapses in the molecular layer (ML), have been shown to be plastic (Jörntell and Ekerot 2002; Rancillac and Crépel 2004). We chose to study whether the PF to Golgi cell synapse shows long-term plastic changes.

Golgi cells (GoCs) are the main inhibitory interneurons of the granule cell layer (GCL), gating the activity of as many as 100 billion granule cells. They typically have a large soma emitting a series of basolateral dendrites in the GCL and three to four long and thin apical dendrites, going into the ML where they branch. In the GCL, GoCs form a large ramified axonal plexus, allowing each cell to contact several thousands GCs (D'Angelo 2008). The central role of the GoC in the cerebellar cortex is exemplified by the extensive interconnections of the cell (Geurts et al. 2003; Watanabe et al. 1998). GoCs receive excitatory inputs from MFs, which form synapses on their basolateral dendrites, from PFs in the molecular layer (in the order of 5,000 inputs per cell) (Ito 2006; Pellionisz and Szentágothai 1973), and possibly also from climbing fibers (Shinoda et al. 2000). GoCs also receive inhibitory inputs from stellate and basket cells in the ML and from Lugaro cells in the GCL (Dieudonné and Dumoulin 2000; Palay and Chan-Palay 1974). The main function of the GoCs is to tonically and phasically inhibit GCs by their GABAergic output (Rossi et al. 2003). Apart from GABA, GoCs co-release glycine at their synaptic terminals (Dugué et al. 2005). In vivo, GoCs have an ongoing irregular, low-frequency firing activity and react to afferent stimulation with a burst of action potentials followed by a pause (Tahon et al. 2005; Vos et al. 1999). In vitro, GoCs behave like regular pacemakers and show phase-reset and resonant activity in the “theta” frequency band (i.e., 4–7 Hz) (Forti et al. 2006; Solinas et al. 2007).

Several studies have shown that PF to GoC synapses have functional glutamate receptors of the AMPA, *N*-methyl-D-aspartate (NMDA), and kainate types (Bureau et al. 2000; Dieudonné 1998; Kanichay and Silver 2008; Misra et al. 2000). Their AMPA receptors (AMPA_Rs) are composed of GluR2 subunits, which are characterized by low Ca²⁺ permeability and linear *I/V* relationships (Menuz et al. 2008). The NMDA receptors (NMDA_Rs) contributing to the excitatory postsynaptic currents (EPSCs) evoked by stimulating the PFs have a high conductance, arising from NR2B-containing receptors, and are present both on the synaptic and extrasynaptic membrane. Low-conductance components arising from NR2D-containing receptors are extrasynaptically localized and do not contribute to the EPSC (Misra et al. 2000). Kainate receptors (KA_Rs) have small amplitudes and slow kinetics and summate in response to presynaptic tetanic stimulation, thus allowing the GoC to integrate excitatory inputs at different time scales (Bureau et al. 2000). Metabotropic glutamate receptors (mGlu_Rs) are also

Address for reprint requests and other correspondence: Q. Robberechts, Theoretical Neurobiology, Dept. of Biomedical Sciences, Campus Drie Eiken T5.37, Univ. of Antwerp, Universiteitsplein 1, 2610 Antwerpen, Belgium (E-mail: quinten@tbn.ua.ac.be).

expressed postsynaptically on PF-GoC synapses. Both group I (mGlu_{R1} and 5) and group II (mGlu_{R2} and 3) are expressed, but mGlu_{R2} are the most abundant (Watanabe and Nakanishi 2003) and serve as a histological marker of GoCs (Geurts et al. 2001). Activation of mGlu_{R2} enhances an inward rectifier potassium current, leading to a slow inhibitory postsynaptic current (IPSC) capable of silencing GoC activity after high-intensity PF input (Watanabe and Nakanishi 2003).

Long-term changes at GoC synapses have not been studied previously. A good candidate is the PF-GoC synapse because PF inputs are in general associated with activity-dependent plastic phenomena. Because of its central position in the control of information transfer to Purkinje cells, a change in the synaptic input to the GoC, even if subtle, could have a significant effect on network activity in the GCL. Here we showed that brief trains of high-frequency synaptic activation can induce long-term depression (LTD) of the parallel fiber (PF) excitatory inputs to GoCs. This PF-GoC LTD is shown using induction protocols (IPs) in voltage-clamp (V-clamp) and current-clamp (C-clamp). The PF-GoC LTD induced by a C-clamp IP is further pharmacologically analyzed.

METHODS

Slice preparation and electrophysiology

Parasagittal and coronal cerebellar slices were acutely prepared from Wistar rats (P15–P22) as previously reported (Dugué et al. 2005) and in agreement with institutional, federal, and European ethical guidelines and laws for animal experimentation. Briefly, the brain was quickly removed after decapitation, and 250 μ m tissue slices were cut by a vibratome (VT 1000 S, Leica) in a ice-cold solution containing (in mM) 130 K-gluconate, 15 KCl, 0.5 EGTA, 20 HEPES, and 25 glucose, with pH adjusted to 7.4 by KOH (oxygenated with 100% O₂) (Dugué et al. 2005). Slices were transferred to an incubation chamber, heated at 32°C for \geq 45 min and later stored at room temperature. The artificial cerebrospinal fluid (ACSF) used for slice incubation, storage, and continuous perfusion during the electrophysiological recordings contained (in mM) 125 NaCl, 2.5 KCl, 1.25 NaH₂PO₄, 26 NaHCO₃, 25 glucose, 2 CaCl₂, and 1 MgCl₂ (compensated with 95% O₂-5% CO₂).

Recordings were carried out at room temperature from the soma of GoCs, visually identified by infrared differential interference contrast (DIC) videomicroscopy. The identity of GoCs was routinely assessed using previously established criteria (Dieudonné 1995) and on observation of EPSCs evoked by extracellular stimuli delivered in the molecular layer (ML) (Beierlein et al. 2007; Bureau et al. 2000). Additional morphological confirmation was obtained in a subset of cells ($n = 15$), filled with a low concentration (0.05%) of Lucifer yellow and imaged by epifluorescence.

Giga-seal patch-clamp recordings were obtained, under the whole cell configuration, using 2–3 M Ω borosilicate-glass pipettes. Intracellular solution contained (in mM) 135 potassium gluconate, 10 KCl, 10 HEPES, 0.2 EGTA, 4 Mg-ATP, 0.4 Na₃GTP, and either 10 Na₂-phosphocreatine and 10 sucrose or 14 Na₂-phosphocreatine, with pH 7.25–7.3 titrated with KOH. For experiments in which BAPTA was added to strongly buffer free intracellular calcium, at increasing concentrations (i.e., 10, 20, and 40 mM), the composition of the intracellular solution was adjusted by decreasing the concentration of potassium gluconate (i.e., 135, 90, and 35 mM, respectively). Voltage- and current-clamp recordings were performed with an EPC 10 amplifier (HEKA, Lambrecht, Germany).

See Supplementary Materials and Fig. S1¹ for description of the voltage-clamp methods and results on parasagittal slices. All results

discussed here are from recordings in coronal slices. In coronal slices, C_m was 149 ± 12 pF (range: 34–392 pF; $n = 36$) and R_{in} was 290 ± 24 M Ω (range: 79–708 M Ω ; $n = 36$). These results are in close agreement with Forti et al. (2006).

A theta-glass pipette (1401016, Hilgenberg, Malsfeld, Germany) filled with ACSF, and accommodating two platinum-wires, was used to deliver bipolar extracellular electrical stimuli. This electrode was placed in the lower half of the ML, at lateral distances of 150–300 μ m. The stimulation artifacts were small. To monitor changes in synaptic efficacy, EPSCs were systematically evoked by paired-pulses stimuli with a 50 ms interpulse interval and repeated at a frequency of 0.1 Hz. Current-controlled stimuli had amplitude and duration in the ranges 8–100 μ A and 100–200 μ s, respectively. The stimulation intensity was adjusted so that the equivalent excitatory postsynaptic potential (EPSP) had a peak value of 5–10 mV. GoCs are in general parasagittally organized (Barmack and Yakhnitsa 2008; Sillitoe et al. 2008). However, it was much easier to evoke and obtain EPSCs in the coronal plane where responses \leq 2 nA were not unusual. No more than one or two position adjustments of the stimulating electrode in the ML were necessary.

The LTD induction protocol (IP) consisted of a high-frequency extracellular electrical stimulation (20 pulses at 100 Hz), repeated 30 times with an interval of 2 s. For the C-clamp IP recordings, the cells were held in current clamp during the IP, injecting negative current to hold the cell around -70 mV but allowing the cell to spike freely during the tetanic stimulation. For the V-clamp IP recordings, the cells were held under voltage clamp at -70 mV during the IP.

Data analysis and statistics

Currents were filtered at 2 kHz, digitized at 5 kHz, and acquired using Pulse software (Heka). Data were analyzed off-line using custom-made macros written in Igor Pro (Wavemetrics, Lake Oswego, OR). All group data are reported as means \pm SE and compared statistically using the Student's *t*-test. A significance of $P < 0.05$ was indicated by an asterisk, and a significance of $P < 0.01$ was indicated by two asterisks.

The PPRs were calculated from the ratio of the second EPSCs over the first EPSCs of the baseline EPSCs, during the 10 min before IP and a stable recording period 25–35 min after IP (60 data points each). No corrective measure was applied to the PPR, as for example, taking the mean of second EPSCs over the mean of the first EPSCs of a series of consecutive paired EPSCs to compensate for the increase in variability of the PPR after IP in case of depression of the EPSCs (Kim and Alger 2001; Sims and Hartell 2005).

The main parameter measured to characterize the synaptic responses evoked by extracellular stimulation was the amplitude of the individual EPSCs, although other parameters like the time-to-peak, the slope of the rising-phase, and the decay-phase time constant were computed. An estimate of the charge transfer, corresponding to each EPSC, was also routinely computed by subtracting the time integral of the steady-state current from the time integral of total current during the EPSC.

Pharmacology

Inhibitory synaptic transmission was blocked by bath-applying a cocktail of 10 μ M of SR95531 (gabazine) and 1 μ M strychnine, a GABA_A receptor and glycine-receptor antagonist, respectively. D-(–)-2-amino-5-phosphono-pentanoic acid (D-APV), (S)- α -methyl-4-carboxyphenylglycine [(S)-MCPG] and LY367385 (S)-(+)- α -amino-4-carboxy-2-methylbenzeneacetic acid were also bath-applied to block NMDA receptors, mGlu_R, and mGlu_{R1}, respectively. LY341495 bis-(*O*-aminophenoxy)-*N,N,N',N'*-tetraacetic acid and KT5720 (9*R*,10*S*,12*S*)-2,3,9,10,11,12-hexahydro-10-hydroxy-9-methyl-1-oxo-9,12-epoxy-1*H*-diindolo[1,2,3-*fg*:3',2',1'-*kl*]pyrrolo[3,4-*i*][1,6]benzodiazocine-10-carboxylic acid, hexyl ester were prepared in DMSO as

¹ The online version of this article contains supplemental data.

stock solutions and used to specifically block mGlu_{R2} receptors and protein kinase A (PKA), respectively. Drug application always followed the establishment of the whole cell configuration, preceded the LTD induction protocol and persisted thereafter. All chemicals were obtained from Sigma-Aldrich, Ascent Scientific, or Tocris Cookson.

RESULTS

Characterization of parallel fiber to Golgi cell synapses

Patch-clamp recordings were established at room temperature, under the whole cell configuration, from the soma of visually identified putative GoCs in the GCL of cerebellar slices, prepared from 15 to 22 day old rats. In general, eliciting EPSCs by extracellular stimulation of the PFs further confirmed the identity of the cell recorded, complementing stan-

dard electrophysiological identification criteria (Dieudonné 1995, 1998). In addition, to isolate glutamatergic PSCs, gabazine (10 μ M) and strychnine (1 μ M) were bath applied for the entire duration of the experiment. A schematic representation of the position of the recording and stimulating electrodes in the coronal slice is shown in Fig. 1C.

Characteristic kinetic parameters of the evoked EPSCs are summarized in Table 1. A sample EPSC, average superposed on series of 20 consecutive EPSCs, is shown in Fig. 1A. Paired-pulse stimuli with 50 ms interpulse intervals were systematically used to evoke EPSCs; representative traces and their averages are shown in Fig. 1B. Paired stimulation of PF-GoCs with relative short time intervals led to paired-pulse facilitation (PPF), implying that the release probability of the second EPSC is increased. When systematically characterized,

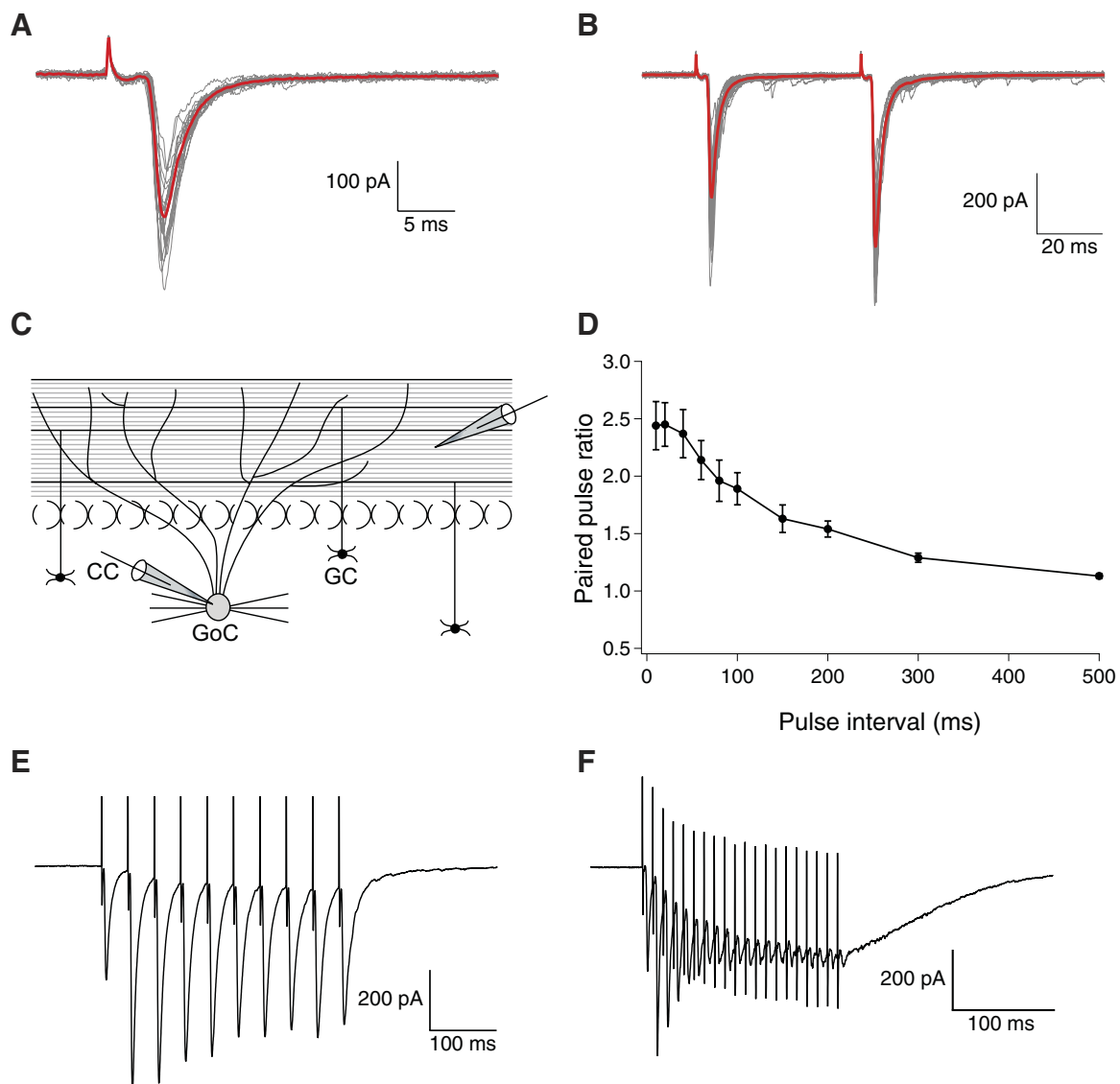


FIG. 1. Properties of parallel fibers to Golgi cell excitatory postsynaptic currents (EPSCs). *A*: representative (gray) and averaged traces (red) from a series of 20 consecutive EPSCs evoked by extracellular stimulation of parallel fibers (PFs) in coronal slices. *B*: in all experiments, EPSCs were evoked with a paired-pulse protocol (10–100 μ A, 100–200 μ s) with a 50 ms interpulse interval. Representative (gray) and averaged (red) traces from 20 consecutive stimulations show paired-pulse facilitation. *C*: schematic diagram of representative positions of the stimulating and recording electrode in the coronal slice plane. *D*: on the average, paired pulse ratios (PPRs) were strongly dependent on the interpulse intervals ($n = 9$; 20 PPRs per data-point, with error bars indicating SE). *E* and *F*: response to tetanic stimulation, averaged over 20 responses, for stimulation at 50 (*E*) and 100 Hz (*F*); the latter was used to induce long-term depression of EPSCs.

TABLE 1. *Passive cell parameters and several EPSC parameters, shown per experimental group and pre- vs. post- induction protocol*

	C-clamp IP (n = 19)	V-clamp IP (n = 7)	NMDAR Block (n = 10)	40 mM BAPTA (n = 9)	Aspecific mGluR (n = 4)	mGluRII Block (n = 7)	mGluRI Block (n = 3)	PKA Block (n = 6)
Rinput, Mohm	271 ± 37	322 ± 52	286 ± 38	255 ± 32	301 ± 61	320 ± 50	573 ± 210	402 ± 61
C _m , pF	131 ± 13	142 ± 46	152 ± 17	96 ± 30	123 ± 25	141 ± 22	62 ± 11	126 ± 22
Amplitude EPSCs, pA								
Pre-IP	243 ± 24	362 ± 51	277 ± 35	263 ± 27	300 ± 104	308 ± 23	279 ± 16	372 ± 40
Post-IP	185 ± 22	253 ± 41	210 ± 36	210 ± 23	284 ± 82	308 ± 39	178 ± 6	361 ± 32
P-value	<0.01	<0.01	0.04	<0.01	0.38	0.86	0.02	0.55
PPR								
Pre-IP	2.06 ± 0.12	2.18 ± 0.17	1.93 ± 0.12	1.96 ± 0.24	2.12 ± 0.40	1.68 ± 0.06	1.75 ± 0.06	1.71 ± 0.2
Post-IP	2.14 ± 0.15	2.34 ± 0.22	2.12 ± 0.16	1.88 ± 0.07	1.81 ± 0.26	1.75 ± 0.14	1.93 ± 0.13	1.70 ± 0.11
P-value	0.57	0.27	0.17	0.24	0.14	0.5	0.10	0.91
Average slope, -pA/ms								
Pre-IP	1.77 ± 0.26	1.77 ± 0.31	1.63 ± 0.38	1.62 ± 0.22	1.14 ± 0.54	1.63 ± 0.15	1.98 ± 0.04	2.64 ± 0.31
Post-IP	1.23 ± 0.22	1.11 ± 0.25	1.28 ± 0.36	1.44 ± 0.26	1.07 ± 0.41	1.68 ± 0.24	1.21 ± 0.1	2.57 ± 0.39
P-value	<0.01	<0.01	0.22	0.44	0.7	0.82	0.04	0.71
Charge transfer, pC								
Pre-IP	1.00 ± 0.08	1.69 ± 0.24	1.16 ± 0.10	1.51 ± 0.19	1.20 ± 0.31	1.24 ± 0.17	1.15 ± 0.08	1.49 ± 0.30
Post-IP	0.81 ± 0.09	1.28 ± 0.25	0.89 ± 0.09	1.10 ± 0.14	1.12 ± 0.22	1.28 ± 0.18	0.77 ± 0.02	1.40 ± 0.26
P-value	<0.01	<0.01	<0.01	<0.01	0.48	0.81	0.03	0.30
Time-to-peak, ms								
Pre-IP	2.01 ± 0.16	2.12 ± 0.21	2.38 ± 0.20	2.56 ± 0.21	2.63 ± 0.41	1.80 ± 0.10	2.08 ± 0.13	1.47 ± 0.22
Post-IP	1.78 ± 0.14	2.09 ± 0.14	2.53 ± 0.27	2.37 ± 0.30	2.68 ± 0.55	1.78 ± 0.08	1.77 ± 0.43	1.49 ± 0.23
P-value	0.15	0.90	0.2	0.54	0.76	0.1	0.41	0.92
Decaytime constant, ms								
Pre-IP	2.95 ± 0.21	2.85 ± 0.22	2.87 ± 0.30	3.26 ± 0.28	2.98 ± 0.74	2.51 ± 0.40	2.66 ± 0.16	2.55 ± 0.20
Post-IP	3.25 ± 0.21	3.01 ± 0.31	2.96 ± 0.30	3.82 ± 0.35	3.03 ± 0.59	2.55 ± 0.37	2.94 ± 0.73	2.43 ± 0.25
P-value	0.08	0.50	0.54	0.26	0.21	0.74	0.25	0.18

PPR, paired pulse ratio. Data are expressed as mean ± SE. Pre-IP means the baseline activity starting 10 min before start IP. Post-IP means the activity 25–35 min after IP. *P* values for statistical significance have been obtained by applying paired *t*-tests between values of the same parameter pre- vs. post-IP.

the paired-pulse ratio (PPRs, i.e., the ratio of the 2nd EPSC amplitude over the 1st EPSC of each pair) decreased exponentially (decay time constant 135 ± 16 ms) for increasing interpulse intervals and leveled off at an average value of 2.45 for intervals <50 ms (Fig. 1D; *n* = 9 cells). The variability of the responses also increased for shorter time intervals. From the traces in Fig. 1D, we estimated a PPR of 2.25 for a time interval of 50 ms between the paired EPSCs.

Responses to trains of stimulations have previously been studied (Bureau et al. 2000; Kanichay and Silver 2008). A detailed study of short-term plasticity of the PF-GoC synapse was done by Beierlein et al. (2007), showing that short stimulus bursts had little overall effect on the strength of the PF-GoC synapse, GoCs do not release endocannabinoids to regulate their PF synapses, and short-term post-tetanic potentiation (PTP) is absent beyond the third pulse. When trains of stimulation pulses were delivered, both short-term facilitation and depression of PF-GoC EPSCs were apparent. Figure 1, *E* and *F*, reports sample average responses to tetani of 10 pulses at 50 Hz and of 20 pulses at 100 Hz, respectively. From Fig. 1F, the progressive depression of EPSC amplitude was particularly prominent at 100 Hz, where separable responses practically vanished by the end of the train.

LTD of the parallel fiber to Golgi cell synapse

We performed extensive preliminary work to study the parameters needed to induce synaptic plasticity at the PF-GoC synapse. In general, we used high-frequency stimulation burst pulses as the IP. This was based on having more consistent results using a high-frequency IP compared with using low-

frequency IPs. More specifically, we used high-frequency, quasi-physiological IPs similar to some IPs used for LTD of the PF-PC synapse where “burst-only” IPs are used and are not necessarily combined with postsynaptic depolarization (Eilers et al. 1997; Hartell 1996). To further increase possible physiological relevancy, we performed the high-frequency IP in coronal slices under C-clamp of the postsynaptic cell, allowing the cell to spike during the IP. Control experiments were done under V-clamp conditions in coronal slices and in parasagittal slices (Supplementary Material and Fig. S1).

During the C-clamp, IP current was applied to hold the membrane potential around -70 mV, although the cell was allowed to spike during the IP stimuli. Quite a regular response developed during the IP, with evoked spiking activity occurring during the first couple of bursts, followed by progressively decreasing postsynaptic and action potentials. By the end of the IP protocol, during the last 5–10 bursts, the extracellular pulses elicited practically no effect on the postsynaptic membrane. This is a result of a complete but transient presynaptic exhaustion of the PFs and/or of postsynaptic receptor desensitization. An example of the response of a cell to the repetitive tetanus is shown in Fig. S2 (Supplementary Material).

Control experiments, where no IP was applied but EPSCs were continuously monitored at 0.1 Hz, showed a moderate decrease of the EPSC amplitude over the 50 min recording period ($-9.9 \pm 3.9\%$ change at $t = 25$ –35 min; *n* = 10; Fig. 2C). No significant changes were seen for the PPR controls (Fig. 2D). The C-clamp IP resulted generally in a progressive and sustained LTD of the amplitude of the evoked EPSCs ($-26.5 \pm 5.1\%$ change at $t = 25$ –35 min after IP; *n* = 19; *P* < 0.01 compared with the control group; Fig. 2, *C* and *F*). This

depression was also reflected by changes in average slope and charge transfer, without any significant changes of kinetic parameters (Table 1). Fifteen of 19 experiments showed a progressive and sustained depression after IP ($-34 \pm 4\%$ change at $t = 25\text{--}35$ min; $n = 15$; Fig. 2B), 3 showed no change, and 1 resulted in clear potentiation of EPSCs amplitude. Of the 15 experiments showing LTD, 8 showed a small and transient post-tetanic potentiation (PTP), 10–20 min after

IP, of the order of 10–30% compared with baseline. Average EPSCs waveforms, before and after IP, are shown in Fig. 2A.

Under the same experimental conditions, changes in the PPR were studied as a potential landmark of alterations in presynaptic release probability. To check whether our recording setup can detect small changes in PPR at distal dendrites and thus be a reliable test for confirming the post- versus presynaptic locus of the plasticity, control experiments were carried out in which the extracellular Ca^{2+} concentration was systematically lowered (see Supplementary Material and Fig. S3). These indicate that, because of the small extent of LTD, any changes in PPR at electrotonically distant sites may be difficult to detect. The C-clamp IP recordings were not associated with a significant increase of the PPR (2.06 ± 0.12 at 10 min before IP vs. 2.14 ± 0.15 at $t = 25\text{--}35$ min after IP; $n = 19$; $P = 0.57$), suggesting a postsynaptic origin of the LTD (Fig. 2E).

To see whether spiking behavior during the C-clamp IP was necessary to induce LTD, we applied the same high-frequency IP while voltage clamping the cell at -70 mV all through the IP. Passive cell parameters and EPSC-related parameters were comparable for the two experimental groups (Table 1). The V-clamp IP results are shown in Fig. 2, C and F ($n = 7$). They showed a similar amount of depression as for the C-clamp IP series ($-29.6 \pm 4.7\%$ change at $t = 25\text{--}35$ min after IP; $n = 7$; $P < 0.01$ compared with the control group). Similar changes were seen for the slope of the rising phase and the charge transfer, whereas kinetic parameters did not show any significant changes (Table 1). A more pronounced PTP was observed in four of the seven recordings and is reflected in the summary plot and in the depression of the PPR right after the IP. No significant changes of the PPR were observed (2.18 ± 0.17 at 10 min before IP vs. 2.34 ± 0.22 at $t = 25\text{--}35$ min after IP; $n = 7$; $P = 0.17$; Fig. 2E), suggesting this IP also has a postsynaptic origin of the LTD.

Using similar IPs as in coronal slices, we performed a number of experiments in parasagittal slices, and these data confirmed that PF-GoC LTD can be evoked in parasagittal slices (see Supplementary Materials and Fig. S1).

Pharmacology of the LTD at the parallel fiber to Golgi cell synapse

Extensive pharmacological studies were done in coronal slices using the C-clamp IP to elucidate the mechanisms involved in LTD induction. Because NMDA_R s are involved in many forms of synaptic plasticity and are expressed at PF-GoC synapses, we tested whether these receptors are needed for

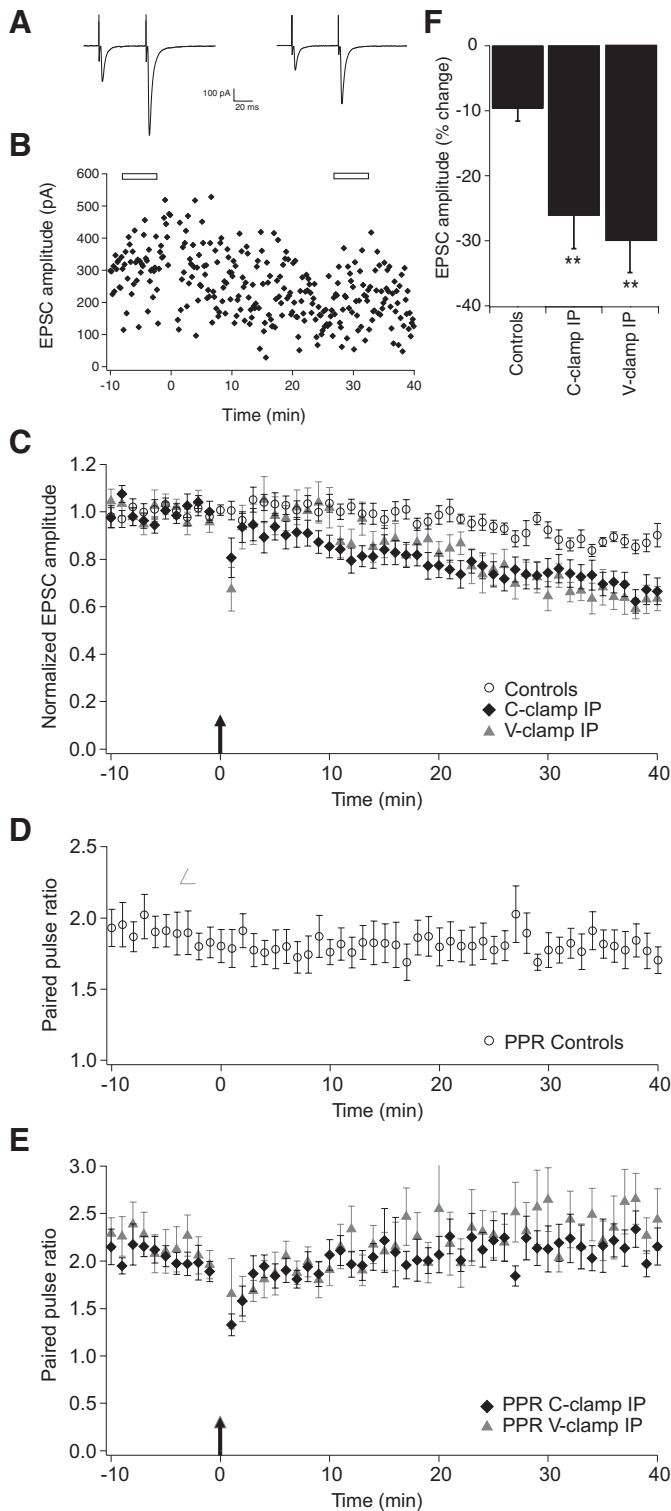


FIG. 2. Long-term depression (LTD) of the parallel fibers to Golgi cells synaptic responses. A: representative averaged traces of evoked EPSCs waveforms 5 min before induction protocol (IP) and 30 min after IP, time points indicated by open bars in B. B: sample experiment showing LTD of EPSCs amplitude evoked by the high-frequency burst IP under current clamp (C-clamp). C: population summary showing the time course of the normalized EPSCs amplitude, comparing control conditions ($n = 10$) with the LTD induced by the high-frequency burst IP under C-clamp ($n = 19$) and voltage clamp (V-clamp) mode ($n = 7$). The arrow at time point 0 indicates the occurrence of the 1 min long IPs. D: population summary of the time course of the PPR for the control condition ($n = 10$). E: population summary of the time course of the PPR for C-clamp IP and V-clamp IP. F: box plot shows that for both C-clamp IP and V-clamp IP protocols the percentage changes of EPSC amplitude averaged over 25–35 min after IP are significantly different from controls (** $P < 0.01$).

PF-GoC LTD. Bath applying 50 μM D-APV from the beginning of the experiment had no significant effect on the PF-GoC LTD (Fig. 3A and Fig. 4) compared with the results summarized in Fig. 2C ($-23.0 \pm 7.6\%$ EPSCs amplitude change at $t = 25\text{--}35$ min; $n = 10$; $P = 0.73$). Again no significant change was present in the PPR time course (1.93 ± 0.12 at 10 min before IP vs. 2.13 ± 0.16 at $t = 25\text{--}35$ min after IP; $n = 10$; $P = 0.17$; Fig. 3A). Under these conditions, 6 of 10 experiments showed LTD, whereas 3 showed no change and 1 experiment showed LTP. A transient PTP was observed in 7 of 10 experiments. This was reflected in a depression of the PPRs, during the same 10 min post-IP period, possibly indicating a presynaptic origin of the PTP. Sample average EPSCs waveforms before and after induction are shown in Fig. 3A. No significant difference was observed, comparing these EPSCs with those evoked without NMDA_R blockade (Table 1). When comparing the population plot of the V-clamp IP experiments (Fig. 2C) with Fig. 3A, a similar time course is observed: a transient PTP over the first 10 min after IP followed by a progression toward sustained depression at ~ 20 min after IP. These results suggest that AMPA_R-mediated EPSCs at PF-GoC synapses undergo NMDA_R-independent LTD but that the extra depolarization caused by NMDA_R activation may cause a faster induction of LTD.

Next, we considered the necessity of an increased intracellular free Ca^{2+} concentration for PF-GoC LTD. Indeed, spiking during C-clamp IP might result in postsynaptic Ca^{2+} transients by Ca^{2+} influx through voltage-gated Ca^{2+} channels, as well as Ca^{2+} release from internal stores. Entry through AMPA_R and NMDA_R could also be possible contributing factors. To test the Ca^{2+} requirement, we first used an intracellular solution containing 10 mM BAPTA (tetraacetic acid). Because this had no effect on the LTD ($-25 \pm 11\%$ change at $t = 25\text{--}35$ min; $n = 4$; $P = 0.94$ compared with results C-clamp IP; Fig. 4), we tested a 20 mM BAPTA concentration for the intracellular solution (BAPTA tetrapotassium salt, with adjustment of the concentration of the potassium gluconate). Under these conditions, no effect on the LTD was observed ($-39 \pm 5\%$ change at $t = 25\text{--}35$ min; $n = 5$; $P = 0.18$ compared with results C-clamp IP; Fig. 4). Because GoC apical dendrites in the ML are very thin, one might expect difficult diffusion of BAPTA to the distant spine-like protrusions that form the postsynaptic part of the PF-GoC synapse, and maybe higher concentrations of the chelating agent are necessary to see an effect on PF-GoC LTD. For this reason, we added 40 mM BAPTA to the intracellular solution and waited longer than usual after establishing the whole cell configuration, before applying the C-clamp IP (40 ± 4 min, $n = 9$, compared with a standard interval 24 ± 2 min, $n = 19$). As in the previous experiments, no significant effect of this Ca^{2+} chelator on LTD was observed ($-19.5 \pm 2.5\%$ change at $t = 25\text{--}35$ min; $n = 9$; $P = 0.23$ compared with results from C-clamp IP and $P = 0.01$ compared with controls; Figs. 3B and 4). The parameters of the EPSCs and passive cell parameters, recorded under these conditions, are summarized in Table 1. These results do not support an essential role for postsynaptic Ca^{2+} transients in PF-GoC LTD induction, although a partial effect is not excluded because LTD induction was slower and less pronounced with 40 mM BAPTA.

Finally, mGlu_Rs are known to be expressed postsynaptically at the PF-GoC synapses. Specifically, activation of mGlu_{R2} by

glutamate gives rise to slow inhibitory postsynaptic potentials through the activation of G protein-coupled inwardly rectifying K^{+} channels (GIRKs) (Knoflach and Kemp 1998; Watanabe and Nakanishi 2003). The mGlu_{R2}-coupling GIRK is predominantly located at GoC dendrites. Because mGlu_Rs are, in general, important mediators for synaptic plasticity phenomena, we studied the effect of blocking these receptors on the PF-GoC LTD.

Because mGlu_{R1} is also expressed in GoCs, although to a lesser degree than mGlu_{R2}, we first did a series of experiments whereby an aspecific mGlu_R blocker [i.e., (S)-MCPG, 500 μM] was bath applied. This resulted in complete blockade of PF-GoC LTD ($-4.8 \pm 4.4\%$ change at $t = 25\text{--}35$ min; $n = 4$; $P < 0.01$ compared with results C-clamp IP; Figs. 3C and 4). No significant change was observed in the PPR, although a rather pronounced but transient decrease in the ratio was recorded after the IP (2.30 ± 0.40 at 10 min before IP vs. 1.77 ± 0.26 at $t = 25\text{--}35$ min after IP; $n = 4$; $P = 0.16$; Fig. 3C).

Next we studied the effect of treatment with a specific mGlu_{R2} blocker (LY341495, 1 μM) in DMSO as vehicle. In this series of experiments, PF-GoC LTD was also completely abolished, confirming the results with the aspecific mGlu_R blocker and emphasizing the role of mGlu_{R2} in PF-GoC LTD ($+0.3 \pm 9.5\%$ change at $t = 25\text{--}35$ min; $n = 7$; $P < 0.05$ compared with results C-clamp IP; Figs. 3D and 4). In six of seven experiments, a PTP was observed, and it was reflected in a depression of the PPRs during the same 10 min post-IP period. Average EPSC waveforms before and after induction are shown in Fig. 3D. This lack of change was also reflected in the other EPSC parameters (Table 1). No significant change was observed in the PPR values (1.68 ± 0.06 at 10 min before IP vs. 1.76 ± 0.14 at $t = 25\text{--}35$ min after IP; $n = 7$; $P = 0.46$; Fig. 3D). Application of the vehicle alone (0.25% DMSO) had no effect on PF-GoC LTD ($-23 \pm 7.1\%$ change at $t = 25\text{--}35$ min; $n = 7$; $P = 0.48$ compared with results C-clamp IP; Fig. 4).

These experiments do not exclude a role of mGlu_{R1} in the induction and/or expression of LTD. We next used the selective mGlu_{R1} antagonist LY367385 at a concentration of 100 μM in the ACSF. No effect on LTD was observed ($-36.0 \pm 2.6\%$ change at $t = 25\text{--}35$ min; $n = 3$; $P = 0.46$ compared with results C-clamp IP; Figs. 3E and 4). No significant change was observed in the PPR (1.75 ± 0.06 at 10 min before IP vs. 1.93 ± 0.13 at $t = 25\text{--}35$ min after IP; $n = 3$; $P = 0.26$; Fig. 3E).

These data confirm an essential role for mGlu_{R2} in the induction and/or expression of PF-GoC LTD. Puzzled by the fact that no clear Ca^{2+} dependency was shown, although an effect on the induction of LTD is not excluded, we tested whether PKA might be a downstream mediator of the induction mechanism for LTD. PKA was chosen because this kinase can be activated without a rise in intracellular Ca^{2+} concentration. As blocker, we used the very selective PKA inhibitor, KT5720, dissolved in DMSO, at a concentration of 0.1 μM in the ACSF. In this series of experiments, PF-GoC LTD was also completely abolished ($-0.3 \pm 4.3\%$ change at $t = 25\text{--}35$ min; $n = 6$; $P < 0.01$ compared with results C-clamp IP; Figs. 3F and 4), suggesting a highly probable role for PKA in the biochemical cascade leading to LTD. In five of six experiments, a PTP was observed, and it was reflected in a depression of the PPRs during the same 10 min post-IP period. Average EPSC wave-

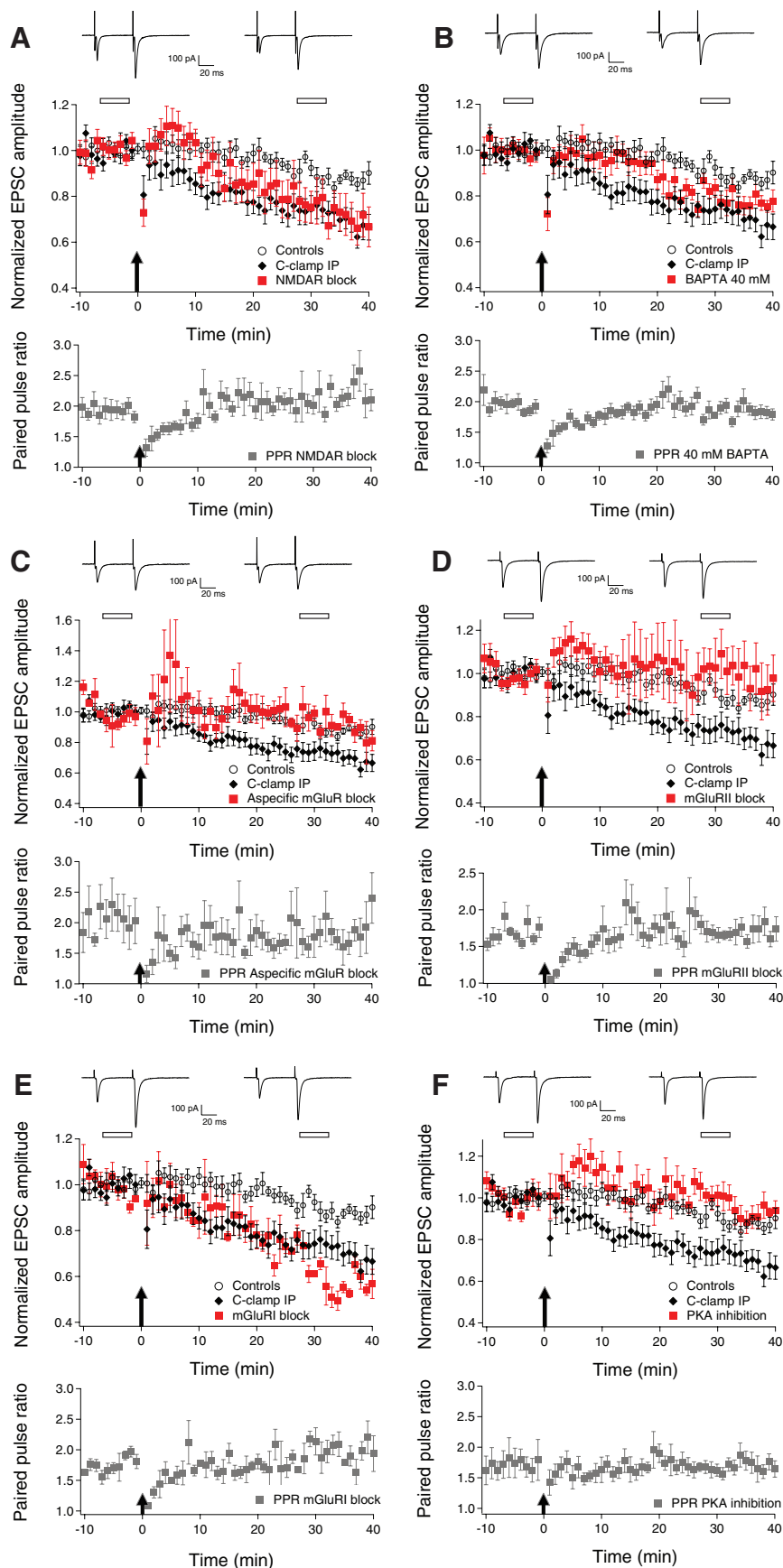


FIG. 3. Pharmacology of LTD at the parallel fibers to Golgi cells synapses. *A–F*: *top*: representative traces of paired EPSCs. Traces shown are the averages of 30 consecutive responses taken from time points indicated by an open bar before and after IP and centered respectively around -5 min before IP and 30 min after IP. *Middle*: time course of the normalized evoked EPSC amplitude under test conditions vs. controls ($n = 10$) and C-clamp IP LTD ($n = 19$). The data for each cell were normalized to the mean value of the EPSC amplitudes 10 min before IP. The arrow at time point 0 indicates the start of the IP lasting 1 min. *Bottom*: time course of the PPR under test conditions. *A*: LTD induced by the C-clamp IP was not blocked in the presence of 50 μ M D-APV ($n = 10$; $P = 0.73$). No significant changes in PPR occurred. *B*: LTD induced by the C-clamp IP was not blocked in Golgi cells (GoCs) loaded with 40 mM BAPTA ($n = 9$; $P = 0.21$), although LTD is clearly slower to develop and the amplitude is smaller than usual. No significant changes in PPR occurred. *C*: LTD induced by the C-clamp IP was completely blocked in the presence of 500 μ M (S)-MCPG ($n = 4$; $P < 0.01$). No significant changes in PPR occurred. *D*: LTD induced by the C-clamp IP was completely blocked in the presence of 1 μ M LY341495 with DMSO as vehicle ($n = 7$; $P < 0.05$). No significant changes in PPR occurred. *E*: LTD induced by the C-clamp IP was not blocked in the presence of 100 μ M LY367385 ($n = 3$; $P = 0.46$). No significant changes in PPR occurred. *F*: LTD induced by the C-clamp IP was completely blocked in the presence of 0.1 μ M KT5720 with DMSO used as vehicle ($n = 7$; $P < 0.05$). No significant changes in PPR occurred.

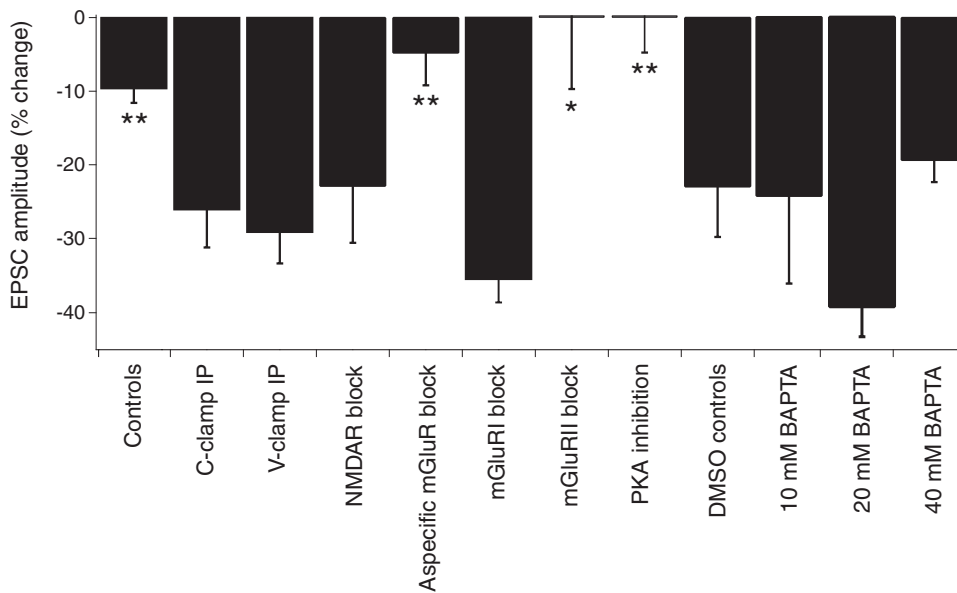


FIG. 4. Box plot summary of all recordings showing the percentage change in EPSC amplitude. Summary showing the percentage change in EPSC amplitude averaged over time 25–35 min after IP, centered around 30 min after IP for the conditions indicated. * $P < 0.05$ and ** $P < 0.01$ compared with C-clamp IP LTD.

forms before and after induction are shown in Fig. 3F. This lack of change was also reflected in the other EPSC parameters (Table 1). No significant change was observed in the PPR values (1.71 ± 0.2 at 10 min before IP vs. 1.70 ± 0.11 at $t = 25\text{--}35$ min after IP; $n = 6$; $P = 0.91$; Fig. 3F).

A summary of all pharmacology experiments is shown in Fig. 4.

DISCUSSION

We reported here for the first time that the PF-GoC synapse can undergo sustained LTD after a quasi-physiological, high-frequency synaptic burst stimulation. PF-GoC LTD was shown to be NMDA_R independent. A clear Ca²⁺ dependence could not be shown. On the other hand, PF-GoC LTD showed a strong dependence on activation of mGlu_R and more specifically on mGlu_{R2}, which are characteristic markers for GoCs. It was also shown that PKA acts as a mediator of PF-GoC LTD. The LTD is likely to be postsynaptically expressed because it was not associated with significant changes in the PPR and because mGlu_{R2} is only postsynaptically expressed.

The central finding of this work is that the PF-GoC synapse can undergo LTD using quasi-physiological IPs similar to those used in PF-PC LTD experiments. This was inspired by the work of Chadderton et al. (2004), showing that sensory stimulations produce short high-frequency bursts of granule cell spikes and the current tendency to use quasi-physiological patterns of stimulation to induce synaptic plasticity in slices (Pugh and Raman 2006; Shin and Linden 2005; Zhang and Linden 2006). No important differences were observed between V-clamp IP- and C-clamp IP-based experiments.

We regularly observed a transient PTP after the IP, sometimes of quite large amplitude and lasting ≤ 20 min. This PTP was more pronounced for the V-clamp IP data than for the C-clamp IP data. It was not excluded that more Ca²⁺ enters the cell during C-clamp IPs because cells were allowed to spike. This could possibly lead to an earlier induction of LTD by itself or through the mediation of other factors necessary for the induction. We cannot exclude, however, that there could be a washout of factors necessary for LTP of the PF-GoC synapse,

which is quite often described for plasticity in hippocampal interneurons (Kullmann and Lamsa 2007).

It is remarkable that protocols similar to IPs used for inducing PF-PC LTD (Coemans et al. 2004; Sims and Hartell 2006) result in LTD of the PF-GoC synapse as well. In the same vein, recent *in vivo* work reported that conjunctive stimulation of peripheral afferents and climbing fibers causes depression of GoC firing activity (Xu and Edgley 2008), but the same peripheral stimulation alone does not cause plasticity of activity. The locus of these plastic changes is unclear but is supposed to lie in the inhibitory input from ML interneurons to GoCs. This represents the first experimental indication of long-term activity changes of GoCs, and it adds to recent literature that the cerebellum is highly prone to plastic changes *in vivo* (Jörntell 2008).

The control experiments done for the V-clamp and C-clamp IP experiments showed a rundown of their activity (about -10% of baseline activity before IP) over the course of the 50 min duration of the experiments. This depression in activity was rather small, and the differences with preIP values were not significant, both for the V-clamp and C-clamp controls. It is not excluded that the stimulation of PFs at a frequency of 0.1 Hz could lead to mild mGlu_{R2} activation and thus be the cause of the moderate depression of activities. This hypothesis is supported by the fact that there is no rundown of the EPSCs in the mGlu_R blocking experiments.

Concerning the induction of PF-GoC LTD, we showed that it is NMDA_R independent. This is also reflected by the lack of effect of APV on the kinetic parameters of the evoked EPSCs. This independence of the PF-GoC LTD is in a way remarkable, because it is generally expected that, if glutamergic synapses express GluR2-containing AMPA_R, they are not permeable to Ca²⁺ and when depolarized they show strong activation of NMDA_R (Kullmann and Lamsa 2007). This did not seem to be the case for Golgi cells because no clear differences were observed when comparing responses to tetanus stimulation with or without NMDA_R blockers. It can of course not be excluded that the NMDA_R conductance undergoes LTD with the same high-frequency IP. Cortical and hippocampal syn-

apses, having a postsynaptic expression of mGlu_{R2} and showing LTD, also show no dependence on NMDA_R for LTD (Otani et al. 2002; Pöschel and Manahan-Vaughan 2005).

An important result of our work is the demonstration that PF-GoC LTD is mGlu_R dependent and more specifically mGlu_{R2} dependent and mGlu_{R1} independent. Postsynaptic mGlu_{R2} endow the GoC with a capability to sense the strength of presynaptic GC inputs. Weak stimuli hardly activate mGlu_{R2}, whereas strong stimuli activate these receptors through spillover activation, causing a temporal inhibition of the GoCs. This permits the GoC to discriminate between weak and strong stimuli (Watanabe and Nakanishi 2003). This mechanism has consequences on the network level activity in the GCL because inhibition will relieve GoC-mediated feedback inhibition in a stimulus-dependent manner (Nakanishi 2009). The fact that blocking the mGlu_{R2} in GoCs leads to relief of LTD of the PF input adds to the important role played by the mGlu_{R2} with regard to the spatiotemporal regulation of the cerebellar circuitry.

The possible role of presynaptically expressed mGlu_{R4} autoreceptors, which are the main group III mGlu_R on PFs, was not studied because of the lack of a specific blocker (Abitbol et al. 2008; Niswender and Conn 2010). LY341495 at 1 μM has no blocking effect on mGlu_{R4} (Johnson et al. 1999; Kingston et al. 1998; Wright et al. 2000). The specific LY341495 block of PF-GoC LTD makes the contribution of a presynaptic mechanism very unlikely because mGlu_{R2} is only postsynaptically expressed and mGlu_{R4} only presynaptically.

We convincingly showed that PKA is involved with the biochemical pathways leading to PF-GoC LTD induction. Group II metabotropic glutamate receptors (mGlu_{R2} and mGlu_{R3}) are known to couple to Gi/o proteins, which inhibit cAMP formation and Ca²⁺ channels at pre- and postsynaptic sites, and they are known to activate GIRK channels at postsynaptic sites (Bellone et al. 2008; Knoflach et al. 2001). Activation of mGlu_{R2} can trigger a form of postsynaptically expressed LTD in different areas of the cortex and hippocampus. At Schaffer collaterals to CA1 synapses, LTD has been shown to be dependent on the simultaneous activation of mGlu_{R2} and A1 adenosine receptors by inhibiting adenylate cyclase, leading to less cAMP and reducing PKA activity (Santschi et al. 2006). Less PKA activity promotes the dephosphorylation and endocytosis of AMPA_R. This mechanism is thus a plausible biochemical mechanism for PF-GoC LTD because a postsynaptic increase in Ca²⁺ does not seem to be necessary.

Although in Marr's seminal theory (1969) it was suggested that only PF-PC synapses should be plastic, plasticity has now been shown in a number of cerebellar synapses (Hansel et al. 2001). Recently, there has been a growing interest in the role of inhibitory interneurons and their relation to synaptic plasticity and circuit control. This is specifically true concerning the role of the GoC in cerebellar motor learning (Dugué et al. 2009; Prsa et al. 2009; Xu and Edgley 2008).

LTD of the PF input on GoCs can have significant effects on the cortical network activity of the cerebellum. GoCs play a central role in the information processing of the cerebellar cortex (Watanabe et al. 1998) by carefully regulating the silencing and the timing of feedback inhibition of GC activity (De Schutter and Bjaalie 2001; Tahon et al. 2005; Vos et al. 1999) and by probably generating regular synchronous oscil-

lations over large GCL fields (D'Angelo 2008; Maex and De Schutter 1998). It is assumed that this oscillatory behavior plays a central role in precise timing of sensorimotor information (Isope et al. 2002) and cognition and memory consolidation by interacting with, for example, the long-term plasticity at the input stage of the cerebellar cortex (D'Angelo et al. 2009). Recent studies show that GoCs are extensively coupled through electrical synapses and display low-frequency oscillatory synchronization, imposing rhythmic inhibition onto GCs (Dugué et al. 2009). PF-GoC LTD can be envisaged to have a pronounced effect on these oscillations and the timing of feedback inhibition.

PF synapses have a low initial probability of release of glutamate (leading to PPF) and can thus function as high-pass filters that allow the GoC easily to detect bursts in presynaptic activity (Abbott and Regehr 2004; Beierlein et al. 2007). PF-GoC LTD induced after intense presynaptic stimulation could lead to a diminishment of inhibition at the input stage and could thus allow more activation of PCs in the corresponding cortical field on a longer time scale.

We used a synchronous but dispersed stimulation IP, which is a physiologically probable input pattern. Therefore PF-GoC LTD can serve as an example of use-dependent changes evoked in a relative small number of synapses with possible consequences for the activity of an entire network of interconnected neurons.

ACKNOWLEDGMENTS

We thank Drs. P. Achard, S. Dieudonné, C. Hansel, B. Barbour, D. Gall, M. de Ruyter, and A. Artola for useful advice and help.

GRANTS

This work was supported by FWO Grants G0450.03 and G.0097.04 and by the University Antwerp (GOA-BOF2004).

DISCLOSURES

No conflicts of interest, financial or otherwise, are declared by the author(s).

REFERENCES

- Abbott LF, Regehr WG.** Synaptic computation. *Nature* 431: 796–803, 2004.
- Abitbol K, Acher F, Daniel H.** Depression of excitatory transmission at PF-PC synapse by group III metabotropic glutamate receptors is provided exclusively by mGlu_{R4} in the rodent cerebellar cortex. *J Neurochem* 105: 2069–2079, 2008.
- Albus JS.** A theory of cerebellar function. *Math Biosci* 10: 25–61, 1971.
- Barmack NH, Yakhnitsa V.** Functions of interneurons in mouse cerebellum. *J Neurosci* 28: 1140–1152, 2008.
- Beierlein M, Fioravante D, Regehr WG.** Differential expression of post-tetanic potentiation and retrograde signaling mediate target dependent short-term synaptic plasticity. *Neuron* 54: 949–959, 2007.
- Bellone C, Lüscher C, Mameli M.** Mechanisms of synaptic depression triggered by metabotropic glutamate receptors. *Cell Mol Life Sci* 65: 2913–2923, 2008.
- Bureau I, Dieudonné S, Coussen F, Mulle C.** Kainate receptor-mediated synaptic currents in cerebellar Golgi cells are not shaped by diffusion of glutamate. *Proc Natl Acad Sci USA* 97: 6838–6843, 2000.
- Chadderton P, Margrie TW, Häusser M.** Integration of quanta in cerebellar granule cells during sensory processing. *Nature* 428: 856–860, 2004.
- Coesmans M, Weber JT, De Zeeuw CI, Hansel C.** Bidirectional parallel fiber plasticity in the cerebellum under climbing fiber control. *Neuron* 44: 691–700, 2004.
- D'Angelo E.** The critical role of Golgi cells in regulating spatio-temporal integration and plasticity at the cerebellum input stage. *Front Neurosci* 2: 35–46, 2008.

- D'Angelo E, Koekoek SK, Lombardo P, Solinas S, Ros E, Garrido J, Schonewille M, De Zeeuw CI. Timing in the cerebellum: oscillations and resonance in the granular layer. *Neuroscience* 162: 805–815, 2009.
- D'Angelo E, Rossi P, Gall D, Prestori F, Nieuws T, Maffei A, Sola E. Long-term potentiation of synaptic transmission at the mossy fiber–granule cell relay of cerebellum. *Prog Brain Res* 248: 71–80, 2004.
- De Schutter E, Bjaalie JG. Coding in the granular layer of the cerebellum. *Prog Brain Res* 130: 279–296, 2001.
- Dieudonné S. Glycinergic synaptic currents in Golgi cells of the rat cerebellum. *Proc Natl Acad Sci USA* 92: 1441–1445, 1995.
- Dieudonné S. Submillisecond kinetics and low efficacy of parallel fibre–Golgi cell synaptic currents in the rat cerebellum. *J Physiol* 510: 845–866, 1998.
- Dieudonné S, Dumoulin A. Serotonin-driven long-range inhibitory connections in the cerebellar cortex. *J Neurosci* 20: 1837–1848, 2000.
- Dugué GP, Brunel N, Hakim V, Schwartz E, Chat M, Lévesque M, Courtemanche R, Léna C, Dieudonné S. Electrical coupling mediates tunable low-frequency oscillations and resonance in the cerebellar Golgi cell network. *Neuron* 61: 126–139, 2009.
- Dugué GP, Dumoulin A, Triller A, Dieudonné S. Target-dependent use of coreleased inhibitory transmitters at central synapses. *J Neurosci* 25: 6490–6498, 2005.
- Eilers J, Takechi H, Finch EA, Augustine GJ, Konnerth A. Local dendritic Ca^{2+} signaling induces cerebellar long-term depression. *Learn Mem* 4: 159–168, 1997.
- Forti L, Cesana E, Mapelli J, D'Angelo E. Ionic mechanisms of autorhythmic firing in rat cerebellar Golgi cells. *J Physiol* 574: 711–729, 2006.
- Geurts FJ, De Schutter E, Dieudonné S. Unraveling the cerebellar cortex: cytology and cellular physiology of large-sized interneurons in the granular layer. *Cerebellum* 2: 290–299, 2003.
- Geurts FJ, Timmermans J, Shigemoto R, De Schutter E. Morphological and neurochemical differentiation of large granular layer interneurons in the adult rat cerebellum. *Neuroscience* 104: 499–512, 2001.
- Hansel C, Linden DJ. Long-term depression of the cerebellar climbing fiber–Purkinje neuron synapse. *Neuron* 26: 473–482, 2000.
- Hansel C, Linden DJ, D'Angelo E. Beyond parallel fiber LTD: the diversity of synaptic and non-synaptic plasticity in the cerebellum. *Nat Neurosci* 4: 467–475, 2001.
- Hartell NA. Strong activation of parallel fibers produces localized calcium transients and a form of LTD that spreads to distant synapses. *Neuron* 16: 601–610, 1996.
- Iansek R, Redman SJ. An analysis of the cable properties of spinal motoneurons using a brief intracellular current pulse. *J Physiol* 231: 613–636, 1973.
- Isope P, Dieudonné S, Barbour B. Temporal organization of activity in the cerebellar cortex: a manifesto for synchrony. *Ann NY Acad Sci* 978: 164–174, 2002.
- Ito M. *The Cerebellum and Neural Control*. New York: Raven Press, 1984.
- Ito M. Cerebellar long-term depression: characterization, signal transduction, and functional roles. *Physiol Rev* 81: 1143–1195, 2001.
- Ito M. Cerebellar circuitry as a neuronal machine. *Prog Neurobiol* 78: 272–303, 2006.
- Ito M, Kano M. Long-lasting depression of parallel fiber–Purkinje cell transmission induced by conjunctive stimulation of parallel fibers and climbing fibers in the cerebellar cortex. *Neurosci Lett* 33: 253–258, 1982.
- Johnson BG, Wright RA, Arnold MB, Wheeler WJ, Ornstein PL, Schoepp DD. [3H]-LY341495 as a novel antagonist radioligand for group II metabotropic glutamate (mGlu) receptors: characterization of binding to membranes of mGlu receptor subtype expressing cells. *Neuropharmacology* 38: 1519–1529, 1999.
- Jörntell H. Input-output plasticity of peripheral responses in cerebellar Golgi cells. *in vivo*. *J Physiol* 586: 4789, 2008.
- Jörntell H, Ekerot CF. Reciprocal bidirectional plasticity of parallel fiber receptive fields in cerebellar Purkinje cells and their afferent interneurons. *Neuron* 34: 797–806, 2002.
- Jörntell H, Hansel C. Synaptic memories upside down: bidirectional plasticity at cerebellar parallel fiber–Purkinje cell synapses. *Neuron* 52: 227–238, 2006.
- Kanichay RT, Silver RA. Synaptic and cellular properties of the feedforward inhibitory circuit within the input layer of the cerebellar cortex. *J Neurosci* 28: 8955–8967, 2008.
- Kim J, Alger BE. Random response fluctuations lead to spurious paired-pulse facilitation. *J Neurosci* 21: 9608–9618, 2001.
- Kingston AE, Ornstein PL, Wright RA, Johnson BG, Mayne NG, Burnett JP, Belagaje R, Wu S, Schoepp DD. LY341495 is a nanomolar potent and selective antagonist of group II metabotropic glutamate receptors. *Neuropharmacology* 37: 1–12, 1998.
- Knoflach F, Kemp JA. Metabotropic glutamate group II receptors activate a G-protein-coupled inwardly rectifying K^+ current in neurons of the rat cerebellum. *J Physiol* 509: 347–354, 1998.
- Knoflach F, Woltering T, Adam G, Mutel V, Kemp JA. Pharmacological properties of native metabotropic glutamate receptors in freshly dissociated Golgi cells of the rat cerebellum. *Neuropharmacology* 40: 163–169, 2001.
- Koekoek SKE, Hulscher HC, Dortland BR, Hensbroek RA, Elgersma Y, Ruigrok TJH, De Zeeuw CI. Cerebellar LTD and learning-dependent timing of conditioned eyelid responses. *Science* 301: 1736–1739, 2003.
- Kullmann DM, Lamsa KP. Long-term synaptic plasticity in hippocampal interneurons. *Nat Rev Neurosci* 8: 687–699, 2007.
- Maex R, De Schutter E. Synchronization of Golgi and granule cell firing in a detailed network model of the cerebellum granule cell layer. *J Neurophysiol* 80: 2521–2537, 1998.
- Marr D. A theory of cerebellar cortex. *J Physiol* 202: 437–470, 1969.
- McCormick DA, Thompson RF. Cerebellum: essential involvement in the classically conditioned eyelid response. *Science* 223: 296–299, 1984.
- Medina JF, Mauk MD. Computer simulation of cerebellar information processing. *Nat Neurosci* 3: 1205–1211, 2000.
- Menuez K, O'Brien JL, Karmizadegan S, Brecht DS, Nicoll RA. TARP redundancy is critical for maintaining AMPA receptor function. *J Neurosci* 27: 8740–8746, 2008.
- Misra C, Brickley SG, Farrant M, Cull-Candy SG. Identification of subunits contributing to synaptic and extrasynaptic NMDA receptors in Golgi cells of the rat cerebellum. *J Physiol* 524: 147–162, 2000.
- Nakanishi S. Genetic manipulation study of information processing in the cerebellum. *Neuroscience* 162: 723–731, 2009.
- Niswender CM, Conn PJ. Metabotropic glutamate receptors: physiology, pharmacology, and disease. *Annu Rev Pharmacol Toxicol* 50: 295–322, 2010.
- Otani S, Daniel H, Takita M, Crépel F. Long-term depression induced by postsynaptic group II metabotropic glutamate receptors linked to phospholipase C and intracellular calcium rises in rat prefrontal cortex. *J Neurosci* 22: 3434–3444, 2002.
- Palay SL, Chan-Palay V. *Cerebellar Cortex*. New York: Springer, 1974.
- Pellionisz A, Szentágothai J. Dynamic single unit stimulation of a realistic network model. *Brain Res* 49: 83–99, 1973.
- Pöschel B, Manahan-Vaughan D. Group II mGluR-induced long term depression in the dentate gyrus in vivo is NMDA receptor-independent and does not require protein synthesis. *Neuropharmacology* 49: 1–12, 2005.
- Prsa M, Dash S, Catz N, Dicke PW, Thier P. Characteristics of responses of Golgi cells and mossy fibers to eye saccades and saccadic adaptation recorded from the posterior vermis of the cerebellum. *J Neurosci* 29: 250–262, 2009.
- Pugh JR, Raman IM. Potentiation of mossy fiber EPSCs in the cerebellar nuclei by NMDA receptor activation followed by postsynaptic rebound current. *Neuron* 51: 113–123, 2006.
- Pugh JR, Raman IM. Nothing can be coincidence: synaptic inhibition and plasticity in the cerebellar nuclei. *Trends Neurosci* 32: 170–177, 2009.
- Rancillac A, Crépel F. Synapses between parallel fibers and stellate cells express long-term changes in synaptic efficacy in rat cerebellum. *J Physiol* 554: 707–720, 2004.
- Rossi DJ, Hamann M, Attwell D. Multiple modes of GABAergic inhibition of rat cerebellar granule cells. *J Physiol* 548: 97–110, 2003.
- Santschi LA, Zhang XI, Stanton PK. Activation of receptors negatively coupled to adenylate cyclase is required for induction of long-term synaptic depression at Schaffer collateral–CA1 synapses. *J Neurobiol* 66: 205–219, 2006.
- Shin JH, Linden DJ. An NMDA receptor/nitric oxide cascade is involved in cerebellar LTD but is not localized to the parallel fiber terminal. *J Neurophysiol* 94: 4281–4289, 2005.
- Shinoda Y, Sugihara I, Wu HS, Sugiuchi Y. The entire trajectory of single climbing fiber and mossy fibers in the cerebellar nuclei and cortex. *Prog Brain Res* 124: 173–186, 2000.
- Sillitoe RV, Chung SH, Fritschy JM, Hoy M, Hawkes R. Golgi cell dendrites are restricted by Purkinje cell stripe boundaries in the adult mouse cerebellar cortex. *J Neurosci* 28: 2820–2826, 2008.
- Sims RE, Hartell NA. Differences in transmission properties and susceptibility to long-term depression reveal functional specialization of ascending axon and parallel fiber synapses to Purkinje cells. *J Neurosci* 25: 3246–3257, 2005.

- Sims RE, Hartell NA.** Differential susceptibility to synaptic plasticity reveals a functional specialization of ascending axon and parallel fiber synapses to cerebellar Purkinje cells. *J Neurosci* 26: 5153–5159, 2006.
- Solinas S, Forti L, Cesana E, Mapelli J, De Schutter E, D'Angelo E.** Fast reset of pacemaking and theta-frequency resonance patterns in cerebellar Golgi cells: simulations of their impact *in vivo*. *Front Neurosci* 1: 1–9, 2007.
- Tahon K, Volny-Luraghi A, De Schutter E.** Temporal characteristics of tactile stimuli influence the response profile of cerebellar Golgi cells. *Neurosci Lett* 390: 156–161, 2005.
- Vos BP, Maex R, Volny-Luraghi A, De Schutter E.** Cerebellar Golgi cells in the rat: receptive fields and timing of responses to facial stimulation. *Eur J Neurosci* 11: 2621–2634, 1999.
- Watanabe D, Inokawa H, Hashimoto K, Suzuki N, Kano M, Shigemoto R, Hirano T, Toyama K, Kaneko S, Yokoi M, Moriyoshi K, Suzuki M, Kobayashi K, Nagatsu T, Kreitman RJ, Pastan I, Nakanishi S.** Ablation of cerebellar Golgi cells disrupts synaptic integration involving GABA inhibition and NMDA receptor activation in motor coordination. *Cell* 95: 17–27, 1998.
- Watanabe D, Nakanishi S.** mGluR2 postsynaptically senses granule cell inputs at Golgi cell synapses. *Neuron* 39: 821–829, 2003.
- Wright RA, Arnold MB, Wheeler WJ, Ornstein PL, Schoepp DD.** Binding of [³H](2*S*,1'*S*,2'*S*)-2-(9-xanthylmethyl)-2-(2'-carboxycyclopropyl) glycine ([³H]LY341495) to cell membranes expressing recombinant human group III metabotropic glutamate receptor subtypes. *Naunyn Schmiedebergs Arch Pharmacol* 362: 546–554, 2000.
- Xu W, Edgley SA.** Climbing fibre-dependent changes in Golgi cell responses to peripheral stimulation. *J Physiol* 586: 4951–4959, 2008.
- Zhang W, Linden DJ.** Long-term depression at the mossy fiber-deep cerebellar nucleus synapse. *J Neurosci* 26: 6935–6944, 2006.